Available online at www.sciencedirect.com

ScienceDirect

Catalysis Today 136 (2008) 76–83

CATALYSIS TODAY

www.elsevier.com/locate/cattod

# A DFT study of pseudomorphic monolayer Pt and Pd catalysts for $NO_x$ storage reduction applications

Jelena Jelic, Randall J. Meyer [*]

*Department of Chemical Engineering, University of Illinois at Chicago, 810 South Clinton, Chicago, IL 60607-7000, United States*

---

**Abstract**

Pseudomorphic monolayer catalysts involving Pd and Pt monolayers above late transition metal (TM) hosts (Cu, Ru, Rh, Ag, Ir and Au) were examined for the oxidation of NO with atomic oxygen. It is found that for systems in which the lattice constant of Pt (or Pd) is expanded, the reaction enthalpy is more endothermic and the reaction barrier is higher. Conversely, for systems under compression, $NO_2$ formation is more exothermic and has a lower barrier. These systems were also examined for their thermodynamic stability upon adsorption of NO and oxygen. Although, segregated systems with a pseudomorphic monolayer of Pt and Pd above a transition metal were found to be stable for systems involving Ru, Ir, Rh and Au even in the presence of adsorbates, oxygen was found to be capable of reversing the position of the supported monolayer and the host metal for systems involving Ag or Cu.

*Keywords:* Platinum; Palladium; Alloy; Catalyst; NSR; Density functional theory; $NO_x$

---

## 1. Introduction

Lean $NO_x$ traps or $NO_x$ storage reduction (NSR) systems have been subject of considerable attention recently as the need for more fuel-efficient engines is exacerbated by rising fuel prices. First pioneered by researchers at Toyota [1–4], the $NO_x$ storage catalyst operates under cycling conditions. First, NO reacts with oxygen over a noble metal (usually Pt) to form $NO_2$, which can subsequently adsorb on a storage material [5–13] (usually BaO, forming barium nitrate) until the storage material is filled. Then the reaction condition is abruptly changed with an injection of a reducing agent. The reducing agent reacts with $NO_x$ over the Pt catalyst (or at the catalyst/storage material interface) producing the typical exhaust products $N_2$, $H_2O$, and $CO_2$ (depending upon the reductant). Finally, the condition in the reactor is once again returned to an oxidizing environment and the cycle repeats.

The reliance on platinum as the primary active element is not ideal due to its high cost. Furthermore, NSR catalysts generally require higher Pt loadings than conventional three-way catalysts further increasing their cost. Therefore, ideally one would like to use considerably less Pt (or avoid its use altogether). One strategy would the development of bimetallic catalysts whose properties mimic that of Pt or possibly improve the performance of Pt. Surface science studies of epitaxially grown metal layers on top of a different metal single crystal have revealed that these pseudomorphic monolayers have novel adsorption properties and therefore could potentially serve as a whole new class of catalysts [14–20]. The stability of such structures under reaction conditions is, however, not well known. Adzic and co-workers have made a breakthrough discovery in their attempt to improve fuel cell catalysts based upon computational work by Mavrikakis and co-workers [14]. Mavrikakis's group predicted that monolayer Pt skin above another transition metal (TM) may have an equal or better performance than pure Pt for oxygen reduction, resulting in the potential to dramatically reduce the amount of Pt in the electrode. Adzic's work is the among the first examples of a successful demonstration of catalytic activity of such pseudomorphic monolayer catalysts under realistic reaction conditions.

As a first step toward the goal of finding new NSR catalysts, we begin with a study of Pt (and Pd)-based pseudomorphic monolayer catalysts for the oxidation of NO to $NO_2$ using density functional theory. Schneider and co-workers [21] have studied the oxidation of NO on Pt(1 1 1) and influence of O coverage on reaction enthalpies. Schneider found that while the

---

[*] Corresponding author. Tel.: +1 312 996 4607.
*E-mail address:* rjm@uic.edu (R.J. Meyer).

0920-5861/$ – see front matter © 2008 Elsevier B.V. All rights reserved.
doi:10.1016/j.cattod.2007.12.135

reaction of NO and O is endothermic at low oxygen coverages (0.7 eV at 0.0625 ML), it switches to an exothermic reaction as the coverage of oxygen increases (−0.28 eV at 0.3125 ML). Furthermore, a barrier of 1.25 eV at 1/16 ML coverage indicates that low-temperature $NO_2$ production will be slow, although it can also be lowered by increasing oxygen coverage. Neurock and co-workers [22] compared the formation of $NO_2$ on Pt (1 0 0) with that on Rh(1 0 0) and found that the barrier is even higher (~1.8 eV) on the rhodium surface. Tang and Trout [23] applied the d-band center weighting model by Tang and Trout [24] to find a catalyst (focusing on Pt alloys) which would be active for oxidizing NO to $NO_2$, but relatively inactive for the oxidation of $SO_2$ to $SO_3$. They found that there is a linear relationship between the weighted d-band center with adsorption energy of $SO_2$ in the initial state and the transition state for oxidation. However, there is a change of slope in the adsorption energy of the transition state for NO oxidation versus the weighted d-band center which induces limitations for the theoretical selectivity. Tang and Trout used 2 × 2 unit cells (0.25 ML coverage) for their calculations and obtained a significantly lower (~0.45 eV) barrier for NO oxidation. This is not surprising, given the results from Schneider revealing the strong coverage dependence of this reaction [21]. As mentioned above, the goal of the current research is to find some alloy combination which will lower the barrier to $NO_2$ formation and improve the NSR catalyst's low-temperature efficiency.

## 2. Method

The density functional theory calculations in this work are performed using the Vienna Ab Initio Simulation Package (VASP) [25,26]. A plane-wave basis set with a cutoff energy of 400 eV and ultra-soft Vanderbilt pseudopotentials (US-PP) [27] were employed. The Perdew Wang (PW-91) form of the generalized gradient approximation (GGA) [28] exchange and correlation functional was used in all calculations reported herein. However, a few calculations were performed with the Revised Perdew-Burke-Ernzerhof by Norskov and Hammer as a basis for comparison [29]. Charge analysis was performed using the Bader analysis method developed by Henkelman and co-workers [30].

The (3 × 3) unit cell representing the system (Fig. 1.) is four layers thick consisting of three layers of close-packed (1 1 1) fcc metals (Rh, Ir, Pd, Au, Ag, Cu) or (0 0 0 1) hcp Ru and Pt in surface layer. The two uppermost metal layers were allowed to relax. Approximately five layers of vacuum were used to separate the slabs. The Brillouin zone is sampled with a uniform 5 × 5 × 1 k-point grid [31]. Lattice constants were set to the experimental values. For some calculations a (2 × 2) unit cell with a 7 × 7 × 1 k-point grid and a (4 × 4) unit cell with 3 × 3 × 1 k-point grid (also four layers thick) were used.

Reaction paths and barriers are determined using the climbing nudged elastic band (NEB) method [32]. In the NEB method a reaction coordinate relating initial (O and NO) and final ($NO_2$) states are defined and a set of intermediate states are distributed along the reaction path. Each intermediate state is fully relaxed in the hyperspace perpendicular to the reaction coordinate.

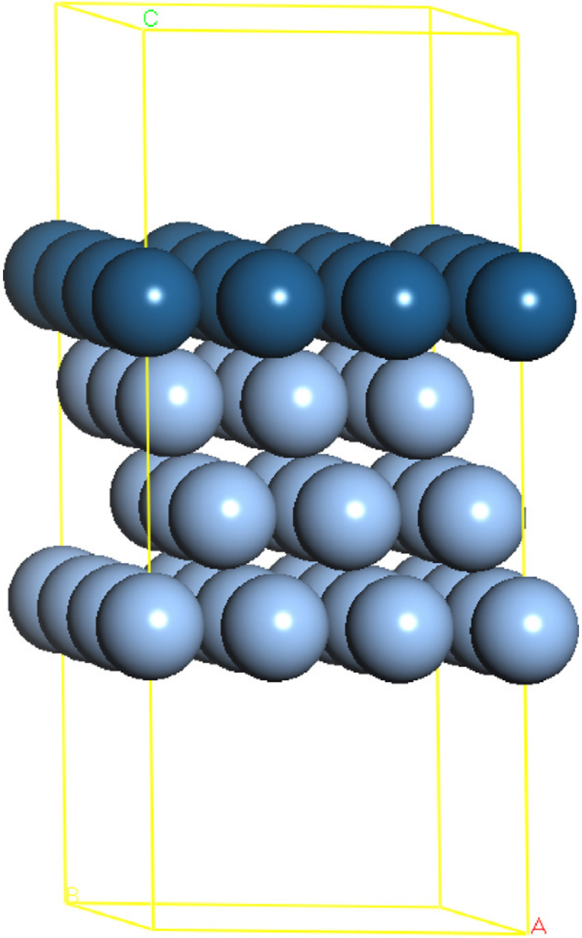

Fig. 1. Example of a psuedomorphic monolayer of Pt over Ag(1 1 1). The (3 × 3) supercell is four layers thick—three layers of the host metal (Rh, Ir, Pd, Au, Ag, Cu, Ru) and a single Pt monolayer on top.

Vibrational frequencies were computed for the initial, transition and final states, where the substrate is frozen and O, NO and $NO_2$ are allowed to vibrate in any direction. If the molecule is in a true transition state it should have one and only one imaginary frequency, corresponding to the addition of O to NO. All adsorption energies and barriers reported include the zero point vibrational energy correction.

## 3. Results and discussion

We begin our examination by choosing alloy catalysts involving Pt and other d-band transition metals (TM) in the neighborhood of Pt: Cu, Rh, Pd, Ag, Ir, Au (all fcc) and Ru (hcp). As Mavrikakis et al. [33], Chen and co-workers [34] and Gross [35] have nicely illustrated, two effects are present in these systems. First, a geometric effect arises due to lattice strain introduced by the epitaxial placement of Pt on the (1 1 1) surface of our host metals and an electronic effect due to the bonding between Pt and the host metal which necessarily has a different electronic configuration than Pt. These two effects then conspire to alter the reactivity of our Pt monolayer giving rise to new catalytic behavior.

Table 1a
Adsorption energies of O, NO and $NO_2$ on (3 × 3) unit cells of Pt pseudomorphic monolayer systems

| | Host metal | | | | | | | |
|---|---|---|---|---|---|---|---|---|
| | Cu | Ru | Rh | Pd | Ag | Ir | Pt | Au |
| O | −0.54 | −0.37 | −0.46 | −1.05 | −1.37 | −0.51 | −0.88 | −1.33 |
| NO | −1.61 | −0.99 | −1.18 | −1.85 | −2.12 | −1.13 | −1.66 | −2.15 |
| $NO_2$ | −1.04 | −0.78 | −0.86 | −1.07 | −0.86 | −0.87 | −1.06 | −1.06 |

Adsorption energies for oxygen, NO and $NO_2$ are listed in Table 1a. For all species, we have examined (3 × 3) cell with 1/9 coverage. The preferred site for oxygen adsorption is found to be the fcc threefold-hollow site. The value for O adsorption is given with respect to molecular $O_2$ not atomic O. However, one can determine the binding energy with respect to atomic oxygen in the gas phase can be determined by simply adding −2.81 eV (half the energy of an $O_2$ bond, $(E_{O_2} - 2E_O)/2$) to the adsorption energy listed in Table 1a. NO adsorbs also on fcc threefold-hollow site, normal to the surface with N down. It should be noted that a small repulsive interaction exists between O and NO when coadsorbed (0.25 eV on Pt(1 1 1)). $NO_2$ adsorbs on bridge site in a μ-*N,O*-nitro configuration as shown in Fig. 2. One N–O bond is essentially parallel with the surface, while another is nearly normal to the surface. Starting structures for $NO_2$ in other adsorption geometries (such as a bidentate-like structure in which $NO_2$ bonds through its oxygen atoms to the surface) located many local minima, but no lower energy structure than the μ-*N,O*-nitro structure was found. Adsorption energies for O, NO and $NO_2$ on Pd–TM systems are presented in Table 1b. Not surprisingly, binding energies of all three adsorbates are slightly higher on the Pd monolayer systems as compared to Pt-based systems.

As has been previously shown [33,36,37], strained metal surfaces have chemical properties that are significantly different from those of unstrained surfaces. The interaction between the adsorbate states and the metal d states is an important part of the interaction energy, and while the sp bands of the metal are broad and structureless, the d-bands are narrow, and small changes in the environment can change the d states and their interaction with adsorbate states significantly. When the lattice is expanded parallel to the surface, the overlap between the d electrons on the neighboring metal atoms decreases, resulting in a simultaneous narrowing of the d-band. Therefore (as described nicely by Hammer in Ref. [37]) to keep the d occupancy fixed, the d states have to move up in energy (for metals with more than half-filled d-bands). The high lying d-band center (close to the Fermi level) implies that antibonding states created by adsorption will lie above the Fermi level—thus they are empty states and lead to strong adsorption.

There is a clear trend in adsorption energies for oxygen and NO on the Pt monolayer systems. Expansion in the lattice results when Pt is placed over Ag and Au, while Pt above other metals results in compression. As a result, NO and O both adsorb more strongly on Pt/Au and Pt/Ag while the adsorption energy is decreased above all other metals except Pd. In the case of Pd, the lattice constant is essentially the same (0.53% compression for Pt/Pd(111)) so any change in the adsorption

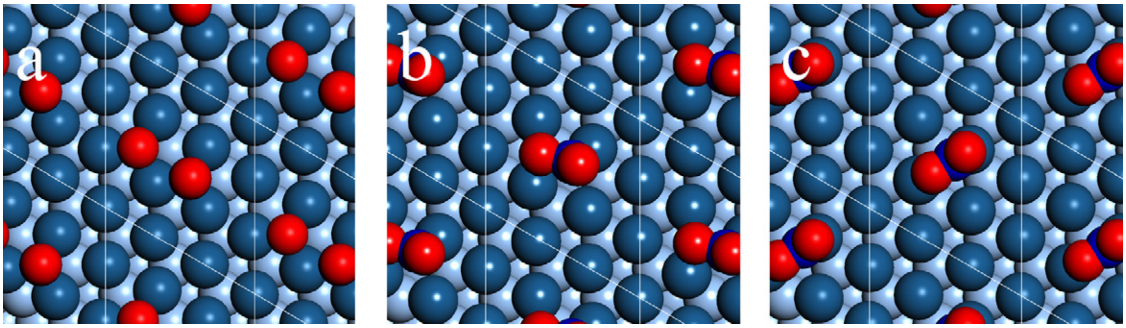

Fig. 2. (a) Top view of initial (O + NO), (b) transition and (c) final ($NO_2$) states.

Table 1b
Adsorption energies of O, NO and $NO_2$ on (3 × 3) unit cells of Pd pseudomorphic monolayer systems

| | Host metal | | | | | | | |
|---|---|---|---|---|---|---|---|---|
| | Cu | Ru | Rh | Pd | Ag | Ir | Pt | Au |
| O | −1.12 | −0.74 | −0.87 | −1.25 | −1.38 | −0.86 | −1.12 | −1.39 |
| NO | −1.86 | −1.32 | −1.69 | −2.21 | −2.34 | −1.63 | −2.04 | −2.39 |
| $NO_2$ | −1.12 | −0.93 | −1.03 | −1.22 | −1.15 | −1.05 | −1.21 | −1.25 |

Table 2a
Bader charge analyses for NO and $NO_2$ molecules adsorbed on Pt pseudomorphic monolayer systems

| | Host metal | | | | | | | |
|---|---|---|---|---|---|---|---|---|
| | Cu | Ru | Rh | Pd | Ag | Ir | Pt | Au |
| NO | 0.37 | 0.42 | 0.42 | 0.49 | 0.51 | 0.40 | 0.48 | 0.50 |
| $NO_2$ | 0.31 | 0.41 | 0.36 | 0.38 | 0.40 | 0.40 | 0.38 | 0.39 |

Table 2b
Bader charge analyses for NO and $NO_2$ molecules adsorbed on Pd pseudomorphic monolayer systems

| | Host metal | | | | | | | |
|---|---|---|---|---|---|---|---|---|
| | Cu | Ru | Rh | Pd | Ag | Ir | Pt | Au |
| NO | 0.37 | 0.47 | 0.44 | 0.49 | 0.46 | 0.46 | 0.45 | 0.46 |
| $NO_2$ | 0.36 | 0.48 | 0.45 | 0.42 | 0.46 | 0.47 | 0.43 | 0.45 |

Table 3a
The activation energies ($E_{act}$) and reaction enthalpies ($\Delta H$) for the NO + O reaction for Pt pseudomorphic monolayer systems

| | Host metal | | | | | | | |
|---|---|---|---|---|---|---|---|---|
| | Cu | Ru | Rh | Pd | Ag | Ir | Pt | Au |
| $E_{act}$ | 0.29 | 0.36 | 0.54 | 1.13 | 1.66 | 0.41 | 1.07 | 1.56 |
| $\Delta H$ | −0.58 | −0.81 | −0.57 | 0.25 | 1.12 | −0.55 | 0.06 | 0.94 |

Table 3b
The activation energies ($E_{act}$) and reaction enthalpies ($\Delta H$) for the NO + O reaction for Pd pseudomorphic monolayer systems

| | Host metal | | | | | | | |
|---|---|---|---|---|---|---|---|---|
| | Cu | Ru | Rh | Pd | Ag | Ir | Pt | Au |
| $E_{act}$ | 1.06 | 0.84 | 0.94 | 1.26 | 1.61 | 0.98 | 1.36 | 1.63 |
| $\Delta H$ | 0.04 | −0.07 | 0.13 | 0.55 | 1.07 | 0.10 | 0.56 | 1.06 |

energy must be explained, at least partially, by an electronic effect. In this case, we look to the charge analysis of the system and find that when Pt is adsorbed on the Pd surface it is electron-rich compared to the surface layer of Pt(111) by $0.04e^-$ as charge is pulled from Pd to Pt. The increase in electron density at the surface layer results in a shift of the d-band toward the Fermi level and explains the stronger binding energy of O and NO on Pt/Pd(1 1 1).

Oddly $NO_2$ does not follow the same trend. The adsorption of $NO_2$ on the surface seems largely unaffected by the expansion or contraction of the lattice. The origin of this effect is not well understood. To gain additional insight into this apparent contradiction, Bader charge analysis was performed (shown in Tables 2a and 2b) and used to compare with the results given in Tables 1a and 1b. From the results, we can see that considerable charge transfer from the surface to NO and $NO_2$ occurs. Both molecules are strong electron acceptors and bind to the Pt(1 1 1) surface via charge donation from the surface to molecules [38]. Furthermore in the case of NO, from our charge analysis, it is clear that on surfaces in which the Pt monolayer is in tension, charge transfer is increased (although the magnitude is not large), whereas charge transfer is decreased when the Pt monolayer is in compression. Not surprisingly, stronger adsorption events can be correlated with larger charge transfer from the surface to NO. In the case of $NO_2$, the situation is not so simple. Overall the amount of charge transfer is slightly decreased and differences between surfaces are also diminished. However, from an argument that invokes charge transfer as a primary predictor of adsorption strength, there should still be a clear trend in the adsorption strength on various Pt monlayer surfaces, which is lacking. Getman and Schneider [38] have done detailed analyses of charge transfer for different $NO_x$ species on different sites of Pt(1 1 1) surface. For NO adsorption on the fcc three hollow sites, they find that $0.50e^-$ is transferred from the metal surface to the adsorbate in agreement with our calculation which shows a $0.48e^-$ transfer. For the $NO_2$ (μ-*N,O*-nitrito configuration) their value of $0.45e^-$ transferred from Pt(1 1 1) to $NO_2$ is only somewhat higher than our own finding of $0.38e^-$. However, the small differences in charge transfer are probably simply due to the lower coverage used by Getman and Schneider in their work (1/16 ML coverage). Therefore it remains unclear why $NO_2$ adsorption is not as sensitive to the changes in the d-band center of the metal surface as other adsorbates.

The reaction of O and NO to form $NO_2$ starts with a NO molecule adsorbed in an fcc threefold-hollow site with an oxygen atom in a neighboring fcc threefold-hollow site so that all fragments are in their energetically preferred sites. The reaction proceeds with NO molecule diffusing towards the adsorbed O atom via a bridge site and O atom diffusing towards NO molecule via the other bridge site. In the transition state O atom is added to the NO molecule and is still in bridge position (Fig. 2, center). Then, added oxygen moves toward Pt atom until the final position is reached, the μ-*N,O*-nitro configuration for $NO_2$.

The activation energies and reaction enthalpies for $NO_2$ formation on different surfaces are listed in Table 3a (Pt systems) and Table 3b (Pd systems). The activation energies are smaller and reactions are more exothermic on surfaces with compressed lattice parameter while on surfaces with an expanded lattice, the reaction is more endothermic and has a high barrier. In fact, we find that the activation energy and the reaction enthalpy are correlated, following the well-established trend first described by Bronsted and later by Evans and Polyani. This correlation known as the Brønsted–Evans–Polanyi (BEP) [39–41] relationship is an empirically derived expression which states that there is a linear relationship between the activation energy and the reaction energy (enthalpy) for an elementary reaction on the surface of the catalyst given below.

$$E_{act} = A + B\,\Delta H$$

We have therefore created BEP plots for NO oxidation on different surfaces for Pt systems and for Pd systems shown in Figs. 3 and 4. The data imply that in the low-coverage regime, the rate-limiting step for $NO_2$ formation is the activation of strongly bound NO and O but may switch to $NO_2$ desorption for some systems involving compressed monolayers of Pd and Pt. As can be noticed from the plot, Pt/Cu and Pd/Cu do not follow this relationship as closely implying that the transition state for

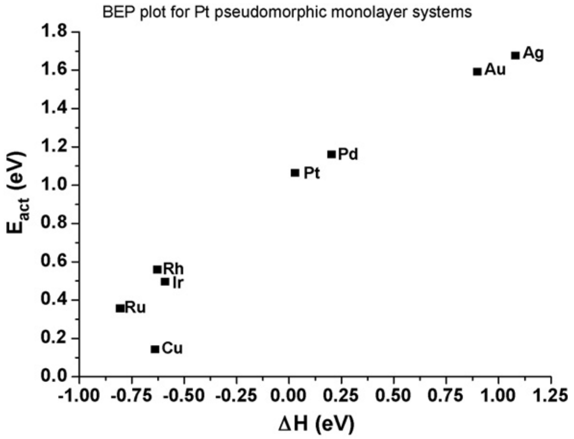

Fig. 3. BEP plot for oxidation of NO on Pt pseudomorphic monolayer systems. The labels refer to the host metal.

$NO_2$ formation on these surfaces is slightly different. This is not highly surprising given that these systems have a much higher degree of strain (~7% compressive strain) which results in some degree of surface buckling and thereby alters how the adsorbates (and the transition state) are bonded to the surface.

A set of calculations were performed using the RPBE functional indicating that both the reactants and products were less strongly bound and that the reaction enthalpy changed from 0.06 eV to −0.16 eV on Pt(1 1 1) at 1/9 ML coverage. Similarly, the reaction barrier was lowered from 1.07 eV to 0.96 eV when the RPBE functional was used. As a final check on the sensitivity of our calculations, a few calculations were also performed using PAW pseudopotentials (but with the PW-91 correlation and exchange functional) [42,43]. The reaction enthalpy was found to be 0.13 eV and the reaction barrier rose to 1.13 eV.

As Schneider and co-workers [21] have observed previously, the reaction possesses a strong coverage dependence. On Pt(1 1 1) we find the reaction goes from $\Delta H = 0.48$ eV at 1/16 ML coverage of O and NO to $\Delta H = -0.71$ eV at 0.25 ML coverage. Similarly, the reaction barrier falls from 1.49 eV at 1/16 ML coverage to 0.47 eV at 0.25 ML. Once again this suggests that the rate-limiting step may no longer be the reaction of NO and O in the high-coverage regime.

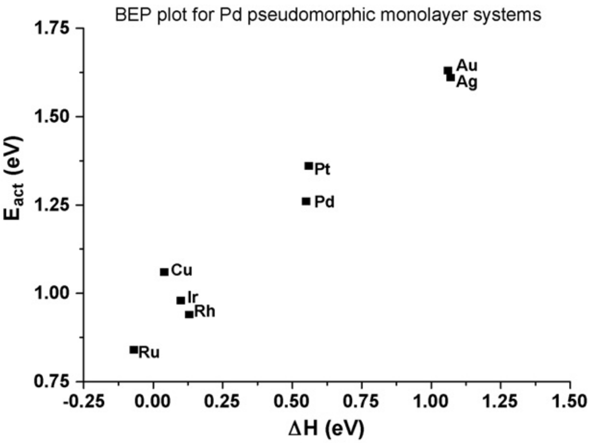

Fig. 4. BEP plot for oxidation of NO on Pd pseudomorphic monolayer systems. The labels refer to the host metal.

Table 4
The activation energies ($E_{act}$) and reaction enthalpies ($\Delta H$) for Pd pseudomorphic monolayer systems for $O_2$ dissociative adsorption reaction

| | Host metal | | | | | | |
|---|---|---|---|---|---|---|---|
| | Ru | Rh | Pd | Ag | Ir | Pt | Au |
| $E_{act}$ | 0.94 | 0.83 | 0.57 | 0.68 | 0.98 | 0.63 | 0.75 |
| $\Delta H$ | −0.78 | −1.01 | −1.69 | −1.92 | −0.99 | −1.58 | −1.83 |

In fact, the Ribeiro group with theoretical support from Schneider and co-workers has recently reported that $O_2$ dissociation or activation is actually the rate-limiting step over Pt catalysts [12,44]. With regard to this result, we have focused instead on Pd systems, and have calculated the adsorption and dissociation for $O_2$ following the example of Mavrikakis and co-workers [45]. The results are given in Table 4. And for Pd is in good agreement with results from Hafner and co-workers [46] (for 0.5 ML coverage we found $E_{act} = 0.77$ eV, Ref. [46] found a barrier of 0.91 eV). As we can see from Tables 3b and 4, these two reactions, NO oxidation and $O_2$ dissociative adsorption, have opposite trends for the reaction barriers on Pd pseudomorphic monolayer systems. For $O_2$ dissociation reaction barrier is higher for systems with compressed lattice parameter and for NO oxidation barrier is smaller. From these results we can also see that the barriers for $O_2$ dissociation are still smaller than those for NO oxidation for the majority of systems. But as we have seen for NO oxidation, strong coverage effects exist in this system (the barrier falls from 0.77 eV at 0.5 ML to 0.57 eV at 0.22 ML).

Since these pseudomorphic monolayer systems are proposed for oxidation of NO, the stability of these segregated systems [19,47–51] due to the presence of oxygen and other adsorbates must be investigated as well. Alloy catalysts have been examined experimentally in deNO$_x$ applications [52–55]. In many cases, it is observed one metal will be enriched in the surface layer. For example, Bagot et al. have investigated the interactions of NO, $O_2$ and $NO_2$ with Pt–Rh alloy (17.4% Rh) wires using field electron microscopy and found that in the absence of active gases, the alloy material has a Pt-rich surface [54]. However, exposure to NO at 295 K results in rhodium enrichment in the surface layer. Therefore, we have examined the ability of our systems to remain segregated when both O and NO are adsorbed. The segregation energy ($E_{seg}$) is defined as the difference in energy of the system with a Pt atoms on the surface ($E_{Pt–TM}$) and system with a Pt atoms in the sub-layer ($E_{TM–Pt–TM}$) ($E_{seg} = E_{Pt–TM} - E_{TM–Pt–TM}$). If the segregation energy is negative, Pt atoms prefer to be on the surface (it is exothermic for the system to remain segregated) and if $E_{seg}$ is positive, the system is more stable with Pt atoms in sub-layer (it is endothermic to move Pt from the second layer to the first). For these calculations we used a 2 × 2 unit cell with a slab of four layers. Once again, the two bottom layers were held fixed while two upper ones were relaxed.

The second parameter that determines the ability of the segregated system to resist transport of Pt (or Pd) into the bulk is the difference in oxygen adsorption energies of systems with Pt on surface and Pt in sub-layer $\Delta E_{ads} = E_{O/Pt–TM} - E_{O/TM–Pt–TM}$. If the difference in adsorption energies is negative, oxygen

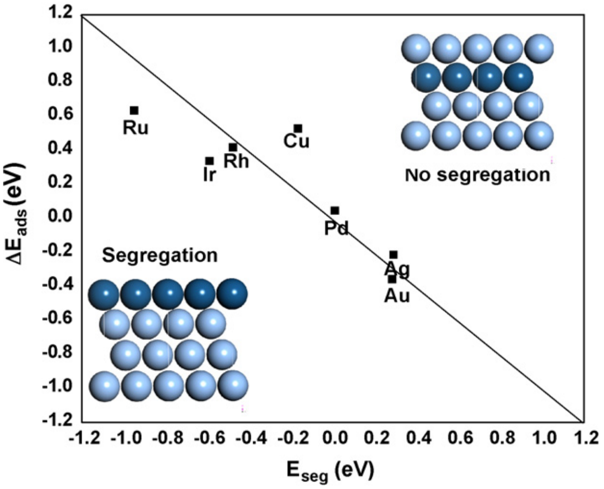

Fig. 5. Segregation energy ($E_{seg}$) vs. adsorption energy difference ($\Delta E_{ads}$) for atomic oxygen on Pt pseudomorphic monolayer systems compared to models where Pt is in the first subsurface layer.

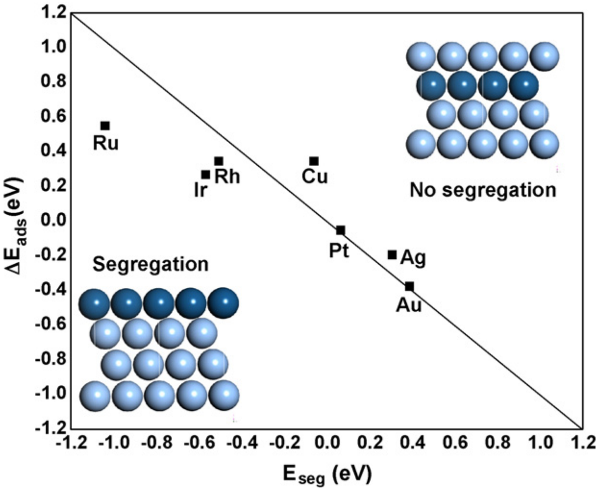

Fig. 7. Segregation energy ($E_{seg}$) vs. adsorption energy difference ($\Delta E_{ads}$) for atomic oxygen on Pd pseudomorphic monolayer systems compared to models where Pd is in the first subsurface layer.

adsorbs stronger on system with Pt on surface and if it is positive, oxygen adsorbs stronger on systems with Pt in sub-layer and induces migration. These two parameters will define stability of systems under oxygen-rich conditions. In general, the adsorption energy difference will have the opposite sign from the segregation energy, as those systems which are favorable in vacuum will often bind oxygen weaker than the less stable, more reactive surfaces as can be seen in Figs. 5–8. Therefore, systems will not remain segregated if the difference in adsorption energies by oxygen is greater than the negative segregation energy ($\Delta E_{ads} > -E_{seg}$). However, if the difference in adsorption energies is less than the negative segregation energy ($\Delta E_{ads} < -E_{seg}$), the system may be thermodynamically stable even under exposure to oxygen. Results for Pt systems are presented in Figs. 5 and 6. Results for Pd systems are given in Figs. 7 and 8.

From the results, it is evident that for systems in which Pt is in compression, Pt will stay at the surface in vacuum, while for the Pt–Ag and Pt–Au systems is opposite is true and Pt would prefer to be in the sub-layer. Menning et al. [48] have investigated the stability of Pt–3d–Pt (1 1 1) (3d = Ti, V, Cr, Mn, Fe, Co, Ni) bimetallic surfaces in vacuum and under an oxygen environment. They found that all the Pt–3d–Pt (1 1 1) systems are stable in vacuum condition. For these systems, the surface d-band was broadened and lowered in energy as compared with Pt resulting in weaker oxygen adsorption energies compared to pure Pt (1 1 1). However, in oxygen-rich conditions, the situation changes. For all Menning's systems O–3d–Pt–Pt structure has lower energy, while in our calculations O binds stronger to Pt than either Ag or Au. O–Ag–Pt–Ag is still stable but in Au system Pt prefers to segregate to the surface. For the other systems (TM = Ir, Rh, Ru), Pt–TM structure is stable under vacuum and for oxygen-rich conditions as well. Only in the case of Cu, Cu–Pt–Cu is considerably more stable in an oxygen-rich environment as the strong binding

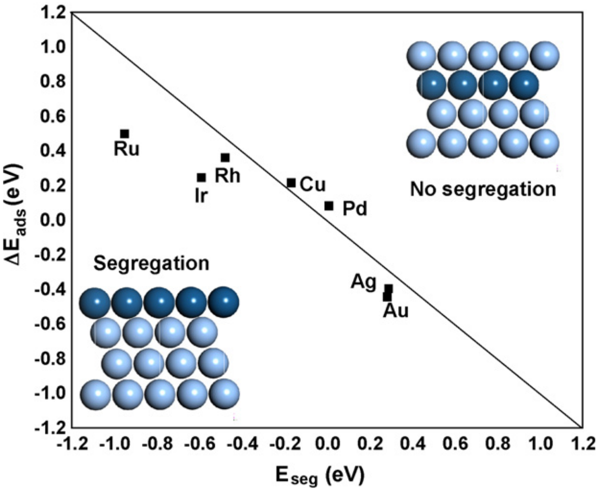

Fig. 6. Segregation energy ($E_{seg}$) vs. adsorption energy difference ($\Delta E_{ads}$) for NO on Pt pseudomorphic monolayer systems compared to models where Pt is in the first subsurface layer.

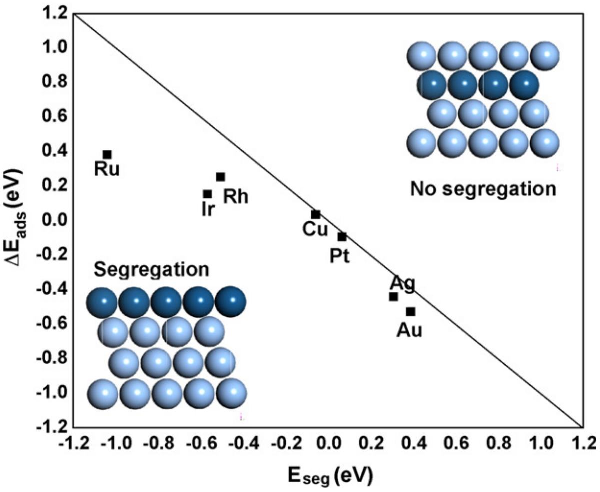

Fig. 8. Segregation energy ($E_{seg}$) vs. adsorption energy difference ($\Delta E_{ads}$) for NO on Pd pseudomorphic monolayer systems compared to models where Pd is in the first subsurface layer.

between Cu and O will overcome the higher surface energy of Cu and will induce transport of Cu to the surface layer. For the Pt–Au system, the oxygen adsorption energy will overcome the higher surface energy of Pt and will keep the Pt on the surface. It is also noteworthy that oxygen adsorption acts as a stronger driving force against segregation (or to induce migration) than NO although the results are not dissimilar. For systems such as Pt/Ir, the results are somewhat promising in that Pt is predicted to remain at the surface even when exposed to our reactants and this system also possesses a smaller barrier for NO oxidation. Segregation is more likely to be stable in Pd systems although their behavior nearly mirrors that of Pt.

We can now compare our results to those of Bagot et al. [54]. Like Bagot et al., we find that the monolayer of Pt is stable over Rh under vacuum conditions. At small NO coverage (0.25 ML) structure with Pt on top layer is still more stable, but the difference is energy of two structures (segregated and non-segregated) is 0.12 eV/atom. At higher coverage (0.5 ML) structure with Rh on top layer is now more stable (in agreement with Bagot et al.). As in our results, Bagot et al. found that that oxygen has a stronger effect on segregation.

However, three additional considerations exist. First there is a kinetic barrier to the diffusion of the host metal to the surface. Menning et al. estimated that diffusion of Co and Ni in Pt had activation energies of 7 kcal/mol and 15 kcal/mol, respectively. Since these barriers will be easily surmounted at the temperatures in the catalytic converter, it should be held as a requirement that our systems are thermodynamically stable. Second, we have considered only a single oxygen coverage (0.25 ML) in our calculations and have not examined other coverages which may influence the ability of a supported monolayer to remain segregated. Furthermore, we have considered that oxygen is chemisorbed, but have not done a full thermodynamic analysis of possible surface oxides which may form nor have we considered the kinetics of the oxide formation process. Surface oxide formation is now well documented in similar systems and could be a factor for host metals which are less noble than Pt [56]. Finally, we have not considered any effects of configurational entropy which would certainly serve to lower the free energy of the system. This is beyond the scope of our current work, but given the lower barriers associated with metal/metal diffusion and the ability of many of these systems to form homogeneous alloys, this should not be ignored (we intend to explore this in future work).

## 4. Conclusion

We have examined of the reaction of O and NO over a series of Pt and Pd pseudomorphic monolayer slabs. Simple BEP relationships can be established which show a direct relationship between the reaction enthalpy and reaction barrier for NO oxidation. For monolayer systems in which the lattice constant was expanded, the resulting barrier was higher than in systems under compression. A simple analysis of the thermodynamic stability of these systems when exposed to oxygen and NO reveals that oxygen will resist segregation (or induce migration) more strongly than NO, but that some of these systems under compression are stable at least from a thermodynamic perspective (of course this does not speak to additional energy gains due to configurational entropy in homogeneous alloys). From our preliminary analysis, Pt/Ir has been identified as a potential system of interest as it is predicted that Pt will remain at the surface even when exposed to our reactants and this system also possesses a smaller barrier for NO oxidation.

Finally, it is important to recognize that the rate-limiting step during the steady state operation of this catalyst may be not the reaction of O and NO on the surface. In a high-coverage regime, other steps may be kinetically important (the kinetics are clearly very sensitive to surface coverage). New experiments examining the activation of oxygen should provide information about the high-coverage regime. In addition, we have confined ourselves to an examination of Pd/Pt supported monolayer catalysts. Of course, homogeneous or intermetallic structures have not been considered here, but should be a part of any serious examination of alloy systems for improving NSR catalysts. Therefore this work is just one piece in the larger puzzle which needs to be solved in order to fully address the replacement of monometallic Pt catalysts in NSR systems.

## Acknowledgement

We gratefully acknowledge funding for this work from the National Science Foundation (Grant #0730937).

## References

[1] S. Matsumoto, Cattech 4 (2004) 102.
[2] M. Takeuchi, S. Matsumoto, Top. Catal. 28 (2004) 151.
[3] N. Takahashi, H. Shinjoh, T. Iijima, T. Suzuki, K. Yamazaki, K. Yokota, H. Suzuki, N. Miyoshi, S. Matsumoto, T. Tanizawa, T. Tanaka, S. Tateishi, K. Kasahara, Catal. Today 27 (1996) 63.
[4] S. Matsumoto, Catal. Today 29 (1996) 43.
[5] W.S. Epling, L.E. Campbell, A. Yezerets, N.W. Currier, J.E. Parks, Catal. Rev. Sci. Eng. 46 (2004) 163.
[6] P. Broqvist, H. Gronbeck, E. Fridell, I. Panas, Catal. Today 96 (2004) 71.
[7] R. Baird, P. Schmitz, J. Phys. Chem. B 106 (2002) 4172.
[8] Y. Sakamoto, K. Okumura, Y. Kizaki, S. Matsunaga, N. Takahashi, H. Shinjoh, J. Catal. 238 (2006) 361.
[9] Y. Su, K.S. Kabin, M.P. Harold, M.D. Amiridis, Appl. Catal. B: Environ. 71 (2007) 207.
[10] J.H. Kwak, D.H. Kim, T. Szailer, C.H.F. Peden, J. Szanyi, Catal. Lett. 111 (2006) 119.
[11] I. Nova, L. Lietti, L. Castoldi, E. Tronconi, P. Forzatti, J. Catal. 239 (2006) 244.
[12] S.S. Mulla, N. Chen, L. Cumaranatunge, G.E. Blau, D.Y. Zemlyanov, W.N. Delgass, W.S. Epling, F.H. Ribeiro, J. Catal. 241 (2006) 389.
[13] L. Cumaranatunge, S.S. Mulla, A. Yezerets, N.W. Currier, W.N. Delgass, F.H. Ribeiro, J. Catal. 246 (2007) 29.
[14] J.L. Zhang, M.B. Vukmirovic, Y. Xu, M. Mavrikakis, R.R. Adzic, Angew. Chem. Int. Ed. 44 (2005) 2132.
[15] T. Jirsak, J. Dvorak, J.A. Rodriguez, Surf. Sci. 436 (1999) L683.
[16] D.E. Beck, J.M. Heitzinger, A. Avoyan, B.E. Koel, Surf. Sci. 491 (2001) 48.
[17] P. Dolle, R. Baudoing-Savois, M. De Santis, M.C. Saint-Lager, M. Abel, J.C. Bertolini, P. Delichere, Surf. Sci. 518 (2002) 1.
[18] J.A. Rodriguez, Surf. Sci. Rep. 24 (1996) 225.
[19] J. Greeley, M. Mavrikakis, Nat. Mater. 3 (2004) 810.
[20] M.B. Zellner, A.M. Goda, O. Skoplyak, M.A. Barteau, J.G. Chen, Surf. Sci. 583 (2005) 281.

[21] S. Ovesson, B.I. Lundqvist, W.F. Schneider, A. Bogicevic, Phys. Rev. B 71 (2005).
[22] D.H. Mei, Q.F. Ge, M. Neurock, L. Kieken, J. Lerou, Mol. Phys. 102 (2004) 361.
[23] H.R. Tang, B.L. Trout, J. Phys. Chem. B 110 (2006) 6856.
[24] H.R. Tang, B.L. Trout, J. Phys. Chem. B 109 (2005) 17630.
[25] G. Kresse, J. Furthmuller, Phys. Rev. B 54 (1996) 11169.
[26] G. Kresse, J. Furthmuller, Comput. Mater. Sci. 6 (1996) 15.
[27] D. Vanderbilt, Phys. Rev. B 41 (1990) 7892.
[28] J.P. Perdew, Y. Wang, Phys. Rev. B 45 (1992) 13244.
[29] B. Hammer, L.B. Hansen, J.K. Norskov, Phys. Rev. B 59 (1999) 7413.
[30] G. Henkelman, A. Arnaldsson, H. Jonsson, Comput. Mater. Sci. 36 (2006) 354.
[31] H.J. Monkhorst, J.D. Pack, Phys. Rev. B 13 (1976) 5188.
[32] G. Henkelman, B.P. Uberuaga, H. Jonsson, J. Chem. Phys. 113 (2000) 9901.
[33] M. Mavrikakis, B. Hammer, J.K. Norskov, Phys. Rev. Lett. 81 (1998) 2819.
[34] J.R. Kitchin, J.K. Norskov, M.A. Barteau, J.G. Chen, Phys. Rev. Lett. 93 (2004).
[35] A. Gross, Top. Catal. 37 (2006) 29.
[36] M. Gsell, P. Jakob, D. Menzel, Science 280 (1998) 717.
[37] B. Hammer, Top. Catal. 37 (2006) 3.
[38] R.B. Getman, W.F. Schneider, J. Phys. Chem. C 111 (2007) 389.
[39] A. Logadottir, T.H. Rod, J.K. Norskov, B. Hammer, S. Dahl, C.J.H. Jacobsen, J. Catal. 197 (2001) 229.
[40] N. Brønsted, Chem. Rev. 5 (1928) 231.
[41] M.G. Evans, N.P. Polanyi, Trans. Faraday Soc. 34 (1938) 11.
[42] P.E. Blochl, Phys. Rev. B 50 (1994) 17953.
[43] G. Kresse, D. Joubert, Phys. Rev. B 59 (1999) 1758.
[44] A.D. Smeltz, R.B. Getman, W.F. Schneider, F.H. Ribeiro, Catal. Today, 2008, this issue.
[45] Y. Xu, A.V. Ruban, M. Mavrikakis, J. Am. Chem. Soc. 126 (2004) 4717.
[46] A. Eichler, F. Mittendorfer, J. Hafner, Phys. Rev. B 62 (2000) 4744.
[47] E.K. Vestergaard, R.T. Vang, J. Knudsen, T.M. Pedersen, T. An, E. Laegsgaard, I. Stensgaard, B. Hammer, F. Besenbacher, Phys. Rev. Lett. 95 (2005).
[48] C.A. Menning, H.H. Hwu, J.G.G. Chen, J. Phys. Chem. B 110 (2006) 15471.
[49] B.C. Han, A. Van der Ven, G. Ceder, B.J. Hwang, Phys. Rev. B 72 (2005).
[50] O.M. Lovvik, Surf. Sci. 583 (2005) 100.
[51] M. Ropo, K. Kokko, L. Vitos, J. Kollar, B. Johansson, Surf. Sci. 600 (2006) 904.
[52] Y. Debauge, M. Abon, J.C. Bertolini, J. Massardier, A. Rochefort, Appl. Surf. Sci. 90 (1995) 15.
[53] K. Tanaka, A. Sasahara, J. Mol. Catal. A: Chem. 155 (2000) 13.
[54] P.A.J. Bagot, A. Cerezo, G.D.W. Smith, Surf. Sci. 601 (2007) 2245.
[55] A. Pietraszek, P. Da Costa, R. Marques, P. Kornelak, T.W. Hansen, J. Camra, M. Najbar, Catal. Today 119 (2007) 187.
[56] K. Reuter, M. Scheffler, Appl. Phys. A: Mater. Sci. Process. 78 (2004) 793.